Role for Phospholipid Interactions in the Trafficking Defect of ΔF508-CFTR†

Ofer Eidelman,‡,§ Shoshana BarNoy,‡,§ Michal Razin,‡ Jiang Zhang,‡ Peter McPhie,|| George Lee,‡ Zhen Huang,⊥ Eric J. Sorscher,⊥ and Harvey B. Pollard*,‡

Department of Anatomy, Physiology, and Genetics, and Institute for Molecular Medicine, USUHS, Bethesda, Maryland 20814, Laboratory of Biochemical Pharmacology, NIDDK, NIH, Bethesda, Maryland 20892, and Departments of Physiology and Medicine, University of Alabama at Birmingham, Birmingham, Alabama 35294

Received April 16, 2002; Revised Manuscript Received July 2, 2002

ABSTRACT: Cystic fibrosis commonly occurs as a consequence of the ΔF508 mutation in the first nucleotide binding fold domain (NBF-1) of CFTR. The mutation causes retention of the mutant CFTR molecule in the endoplasmic reticulum, and this aberrant trafficking event is believed to be due to defective interactions between the mutant NBF-1 domain and other cellular factors in the endoplasmic reticulum. Since the NBF-1 domain has been shown to interact with membranes, we wanted to investigate whether NBF-1 and CFTR interactions with specific phospholipid chaperones might play a role in trafficking. We have found that the recombinant wild-type NBF-1 interacts selectively with phosphatidylserine (PS) rather than phosphatidylcholine (PC). By contrast, NBF-1 carrying the ΔF508 mutation loses the ability to discriminate between these two phospholipids. In cells expressing ΔF508-CFTR, replacement of PC by noncharged analogues results in an absolute increase in CFTR expression. In addition, we detected progressive expression of higher molecular weight CFTR forms. Thus, phospholipid chaperones may be important for CFTR trafficking, and contribute to the pathology of cystic fibrosis.

Cystic fibrosis is the most common lethal autosomal recessive disease in the U.S. population, and is due to mutations in the CFTR[1] gene (*1*−*4*). The most common mutation is a missing phenylalanine at position 508 (ΔF508), which occurs in NBF-1, the first nucleotide binding fold domain. The basis of CF pathology for the [ΔF508]CFTR is believed to be failure of the mutant protein to traffic correctly to the plasma membrane (*5*−*10*). Protein chaperones have been implicated (*11*, *12*). However, recent studies indicate that NBF-1 also interacts with membranes. For example, anion channels are formed in planar acidic phospholipid bilayers by both recombinant wild-type and [ΔF508]-NBF-1 (*13*). More recently, NBF-1 has been shown to behave as a membrane-spanning integral membrane complex when expressed in *E. coli* plasma membranes (*14*), and to span the plasma membrane when expressed in sf9 insect cells (*15*). Furthermore, a recent crystal structure of HisP, a bacterial homologue of the NBF domains of CFTR, has also been interpreted to show a transmembrane structure (*16*). Inasmuch as phospholipid chaperones are critical for proper trafficking of lac permease in *E. coli* (*17*, *18*), we have hypothesized that specific interactions between CFTR and phospholipids might also play a role in the CFTR trafficking process in mammalian cells.

To test this hypothesis in vitro, we have utilized the single tryptophan (W496) in NBF-1 or [ΔF508]NBF-1 as a natural reporter group. We have found that phospholipid membranes cause changes in W496 fluorescence. Furthermore, the fluorescence can be blocked by an aqueous quencher to W496. Finally, phospholipids also differentially change the circular dichroism spectrum of both mutant and wild-type NBF-1 proteins. In wild-type NBF-1, these changes depend specifically on the kind of phospholipid added, with the effect of phosphatidylserine (PS) being much greater than phosphatidylcholine (PC). However, the two lipids become equal in effect in the presence of the ΔF508 mutation. Our data thus indicate that the ΔF508 mutation leads to a profound and dramatic increase in the affinity of NBF-1 for PC.

Based on these data, we hypothesized that the trafficking defect for mutant CFTR might be based on aberrant interactions with PC. Using mouse L-cells expressing [ΔF508]CFTR to test this hypothesis in vivo, we replaced a large fraction of the PC with phospholipid analogues having noncharged headgroups. Under these conditions, we detected substantial increments in total CFTR. In addition, we detected higher molecular weight CFTR bands, suggesting an increase in glycosylation and processing. We interpret these data to suggest that aberrant interactions between the mutant NBF-1 domain of CFTR and phospholipid chaperones may indeed

† This work was funded in part by grants from the NIH (R01-DK-53051) and the Cystic Fibrosis Foundation.

* Address correspondence to this author at the Department of Anatomy, Physiology, and Genetics, Building B, Room B2100, Uniformed Services University School of Medicine, USUHS, 4301 Jones Bridge Rd., Bethesda, MD 20814. TEL: 301-295-3661; FAX: 301-295-2822; Email: hpollard@usuhs.mil.

‡ USUHS.

§ These two individuals contributed equally as first authors on this paper.

|| NIDDK, NIH.

⊥ University of Alabama at Birmingham.

[1] Abbreviations: CF, cystic fibrosis; CFTR, cystic fibrosis transmembrane conductance regulator; NBF, nuclear binding fold; PS, L-α-phosphatidyl-L-serine; PC, L-α-phosphatidylcholine; SUV, small unilamellar vesicles; LUV, large unilamellar vesicles; CD, circular dichroism; AP, 3-amino-1-propanol; AB, 2-amino-1-butanol; MEA, 2-(methylamino)ethanol; ECL, enhanced chemiluminescence; FITC, fluorescein isothiocyanate; TFE, trifluroethanol; SDS, sodium dodecyl sulfate.

10.1021/bi020289s
Published on Web 08/14/2002

contribute to the processing defect identified for the ΔF508 mutant, thereby contributing directly to the cystic fibrosis disease process.

MATERIALS AND METHODS

Preparation and Purification of Recombinant NBF-1 and [ΔF508]NBF-1. NBF-1 (CFTR426−588) and [ΔF508]NBF-1 were prepared as fusion proteins with GST, cleaved by thrombin, and purified by gel electrophoresis as previously described (*13*).

Measurement of Tryptophan Fluorescence. Fluorescence spectra (excitation at 290 nm) were obtained at a protein concentration of 30 μg/mL in the presence or absence of PS or PC small unilamellar vesicles (SUV) at a lipid concentration of 0.1 mM in buffer A (10 mM MES−NaOH, 10 mM HEPES−NaOH, 300 mM sucrose, 1 mM EDTA, pH 6.0), or after incubation in 8 M urea for 25 min at room temperature (22 °C). Spectra were recorded using a SPEX Fluorolog photon counting spectrofluorometer with a 305 nm cutoff filter to eliminate scattering and stray light. Fluorescence intensities were corrected by subtracting the blank measurement without added protein.

Tryptophan Fluorescence Quenching. Protein solutions of 1.5 μM were titrated with acrylamide in the presence or absence of phospholipid vesicles (PS-SUV or PC-SUV, 0.1 mM) in buffer A, or after incubation in 8 M urea for 25 min at room temperature (22 °C). The fluorescence intensity, excitation at 290 nm and emission at 345 nm with a 305 nm cutoff filter, was recorded during titration of the solution with small aliquots of 5 M acrylamide. The effects due to light scattering by the liposomes were corrected by subtracting the corresponding blank signal without added protein. The ratio of the corrected fluorescence intensity in the absence of the quencher, F_o, to the corrected intensity in the presence of the quencher, F, as a function of the quencher concentration, was calculated and plotted as the Stern−Volmer plot. The Stern−Volmer constant is given by the slope of the Stern−Volmer plot.

Preparation of Phospholipid Vesicles. Phospholipids were purchased from Avanti Polar Lipids (Alabaster, AL). Phospholipids were deposited from a chloroform solution as a film by evaporation in a rotary evaporator under an argon atmosphere in a round-bottom flask, and subsequently lyophilized under high vacuum. After hydration with buffer B (10 mM Tris-HCl or 10 mM HEPES−NaOH, 150 mM NaCl, 0.1 mM EDTA, pH 7.4), the solution is thoroughly vortexed. To prepare large unilamellar vesicles (LUV), the suspension is freeze−thawed 5 times and extruded through nucleopore filters (2 × 0.2 μm, 10 × 0.1 μm) in a high-pressure extruder.

Preparation of Small Unilamellar Vesicles (SUV). Small unilamellar vesicles (SUV) were prepared by sonication of vortexed phospholipids under argon for 15 min until clarity using a titanium tip probe sonicator. After sonication, the sample was spun down (3000*g*, 5 min) to remove possible metal particles.

Circular Dichroism. CD spectra of 5 μM NBF-1 (wild-type or mutant) in 10 mM Tris-HCl, pH 7.5, in the presence or absence of 1 mM phospholipid SUV, were collected in a computer-driven Jasco J500C spectropolarimeter, using a quartz 0.1 cm optical path length cell at 25 °C. A mean residue weight (MRW) of 108 was assumed. Spectra were scanned 4 times and averaged. Averaged blank spectra were subtracted to yield the 'pure' protein spectra. Data were converted into units of mean residue ellipticity using the equation:

$$[\Theta] = \frac{\{(\text{defl},m^0) \times 10 \times \text{MRW}\}}{\{\text{conc (mg/mL)} \times \text{path length (cm)} \times 100\}} \quad (1)$$

The β sheet content in aqueous buffer, 30−50%, agrees with the levels predicted by the Chou and Fasman method (*19*). However, the α helical content predicted by the Chou and Fasman method (*19*), ca. 40%, is experimentally obtained only when wild-type or mutant NBF-1 is dissolved in 94% TFE.

Preparation of Large Unilamellar Vesicles (LUV). Vortexed vesicles, prepared as described above in buffer B, were subjected to 5 freeze−thaw cycles of liquid N_2/37 °C, followed by filtration through polycarbonate Nucleopore filters in an extruder apparatus (Lipex Biomembranes, Vancouver, BC). The samples were passed 2−4 times through doubly stacked filters of 0.2 μm pore size, and then 7−10 times through doubly stacked filters of 0.1 μm pore size.

Preparation of Calcein-Loaded LUV. Calcein (fluorexon, indicator grade, Aldrich) was loaded into extruded LUV by adding 1 volume of LUV to 3 volumes of 90 mM calcein (neutralized with NaOH). The suspension was then exposed to 5 freeze−thaw cycles of liquid N_2/37 °C. Untrapped calcein was separated by passing the mixture over a PD10 column (Pharmacia) with buffer B used as the eluant. The fraction with the highest ratio of fluorescence signal increase after addition of detergent (ca. 1/60 volume of 10% NP40) was used in the experiment.

Calcein Efflux Assay. The release of calcein was determined fluorometrically by monitoring the decrease in self-quenching as the dye was released from the vesicles. The conditions on the SPEX fluorolog photon counting spectrofluorometer were excitation at 490 nm and emission at 522 nm, with a 515 nm cutoff filter to eliminate contributions from light scattering and stray light. The kinetic experiments were initiated by injecting wild-type or mutant NBF-1 from a stock solution (0.1 mg/mL in 10 mM Tris-HCl, pH 7.5) into a cuvette containing 2 mL of calcein-loaded LUV in buffer C (10 mM MES−NaOH, 10 mM HEPES−NaOH, 300 mM sucrose, and 2 mM EDTA, pH 6.0) at 37 °C. The fluorescence intensity corresponding to total release of calcein was determined by addition of 30 μL of 10% NP-40. Progress in the reaction was calculated as the percentage of dequenching, using the formula: % dequenching $= F(t) = [(f_t - f_o)/(f_\infty - f_o)] \times 100$, where f_t is the measured fluorescence at time t, f_o is the fluorescence of the loaded vesicles before addition of the protein, and f_∞ is the fluorescence after addition of NP-40. $F(t)$, the normalized fluorescence at time t, was modeled by eq 2 (see text).

Effect of Choline Analogues on CFTR Maturation. Permanently transfected L-cells expressing either wild-type or [ΔF508]CFTR were obtained from Drs. Dan Devor and Ray Frizzel, University of Pittsburgh School of Medicine. Wild-type cells had recently been reselected by SPQ-based flow cytometry, while mutant cells are estimated to be 40% positive producers. Cells were incubated for 2−3 days in

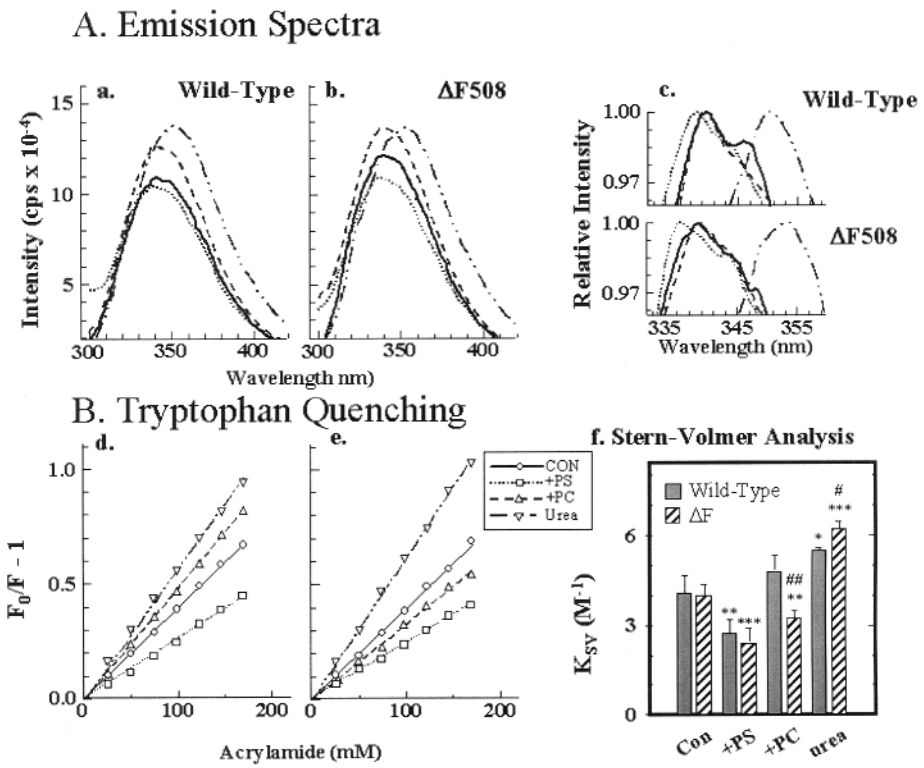

FIGURE 1: Effect of phospholipids on the tryptophan emission spectrum and acrylamide quenching of NBF-1 and NBF-1(ΔF508). (A) Tryptophan fluorescence spectrum of wild-type (a) and mutant ΔF508-NBF-1 (b) in the absence of added phospholipids (—) or in the presence of PS-SUV (•••), PC-SUV (- - -), or 8 M urea (- •• -). (c) NBF-1 fluorescence spectra normalized relative to the respective peak of fluorescence intensity. The upper panel is wild-type NBF-1. The lower panel is NBF-1(ΔF508). Conditions are as described in parts a and b. (B) Quenching of tryptophan fluorescence in recombinant NBF-1 (d) and in mutant NBF-1(ΔF508) (e) in different concentrations of acrylamide. Conditions are as described above. The Stern−Volmer constants (i.e., the slopes of the lines in parts d and e) are shown in part f. Statistics: Data are significantly different from the corresponding control at the 0.05 level (*), the 0.01 level (**), or the 0.001 level (***). Data are significantly different from the respective wild-type at the 0.05 level (#) or the 0.01 level (##).

choline-free DMEM medium (Biofluids, Rockville, MD), supplemented with either 40 μg/mL choline (Sigma) or choline analogues (MEA [2-(methylamino)ethanol]; or AP (3-amino-1-propanol); or AB (2-amino-1-butanol), all from Aldrich Chemical Co.), following the method of Glaser et al. (*20*). According to Glaser et al. (*20*), L-cells are able to survive under these conditions for up to 1 month. Antibodies used to detect CFTR were a monoclonal antibody either to the C-terminal four residues of CFTR (Genzyme) or to an epitope in the NBF-1 domain (gift from Dr. Norbert Kartner, Toronto). Cells were harvested in a protease inhibitor cocktail, and processed for electrophoresis by SDS−PAGE, transblotting, and ECL detection exactly as described by Guay-Broder et al. (*21*). Protein was measured by the BAC method (Pierce).

Immunocytochemistry. L-cells transfected with either wild-type or ΔF508-CFTR were grown on coverslips for 2−3 days in the presence or absence of the indicated concentration of MEA. Cultures were subconfluent at that stage. Cells were fixed with formaldehyde, permeabilized with 0.2% Triton X-100, and treated with glycine. The samples were labeled with monoclonal anti-CFTR (Genzyme, C-terminal epitope) as primary antibodies, and FITC-labeled anti-mouse IgG as secondary antibodies. The coverslips were then glued to microscope slides.

Confocal Microscopy. Cells were imaged on a BioRad X1000 laser scanning confocal microscope using a Zeiss microscope with a 40× objective. *Z*-axis slices were taken at ca. 1.5 μm using a motorized stage. The fluorescence intensities were then converted to false color and superimposed over the phase image of the field.

Laser Scanning Cytometry. The slides were read on a LSC (Boston, MA) Laser Scanning Cytometer. The primary discrimination for identifying cells was obtained from the light-scattering channel and included selection based on the area of the scattering object. The adequacy of these settings was confirmed by observation of the computer-generated contours of included cells against the phase image. A secondary discrimination was employed against cells with very high integrated fluorescence intensity (mainly due to very bright, crystalline spots within the cell contour). The adequacy of this discrimination was confirmed by observing the contours against the FITC fluorescence channel image. Data are shown as histograms of the number of cells vs fluorescence intensity integrated over the cell contour.

RESULTS

Fluorescence Studies of Wild-Type and of Mutant NBF-1 Domains. Figure 1a−c illustrates the changes in fluorescence intensity and emission maximum for wild-type and mutant NBF-1 species in the presence of either phosphatidylserine (PS) or phosphatidylcholine (PC), or the denaturant 8 M urea. The phospholipids PS and PC were chosen as representative components of the cytosolic and luminal leaflets of the endoplasmic reticulum membranes, respectively. The tryptophan emission maximum for the wild-type NBF-1 in buffer was found to be 341.3 ± 0.9 nm ($n = 8$), while that for the

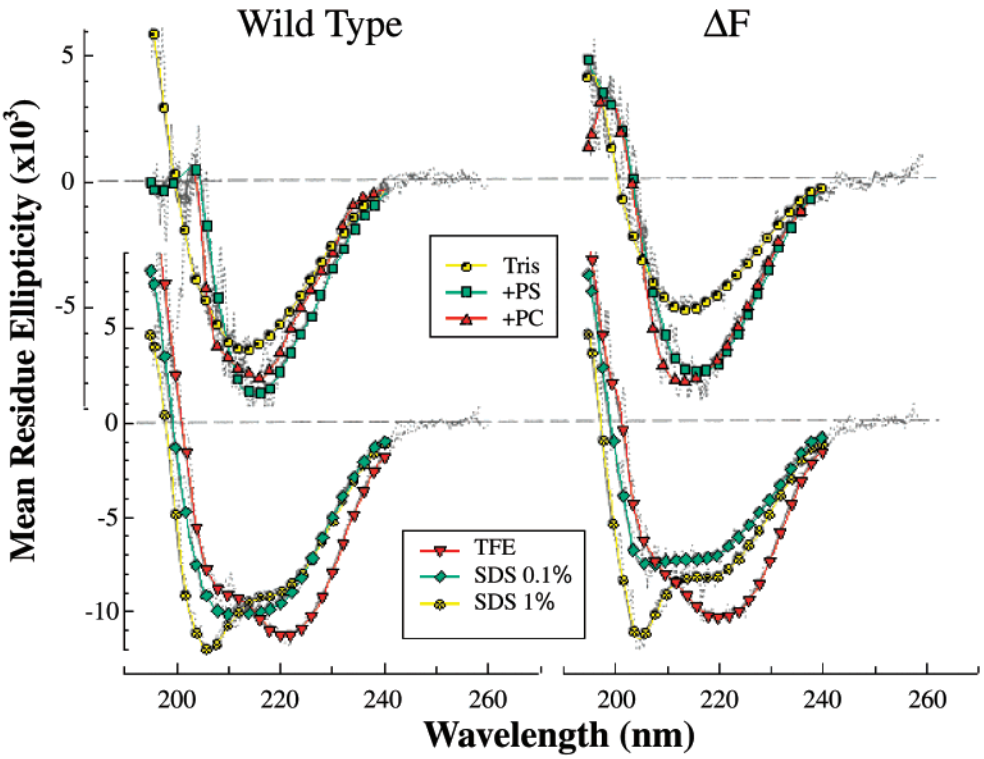

FIGURE 2: Circular dichroism spectra of wild-type and ΔF508-NBF-1. Upper spectra: CD spectra were taken in Tris buffer supplemented with either PS (□), PC (△), or no phospholipids added (⊙). Lower spectra: Solvent effects on the secondary structure of NBF-1 are depicted by the CD spectra in 94% TFE (⊗), 0.1% SDS (◇), and 1% SDS (▽).

ΔF508 mutant was 338.6 ± 1.1 nm (n = 9). These were significantly quenched and blue-shifted from conditions in 8 M urea, in which the wild-type NBF-1 emission maximum was 351 ± 1 nm (n = 2), and that for the mutant NBF-1 was 354 ± 1 nm (n = 2). These results thus indicate that the single tryptophan in each species is located in a naturally hydrophobic environment, and that the two species differ from each other conformationally. A similar general conclusion regarding the hydrophobic tryptophan environment for wild-type and mutant NBF-1 has also been drawn by Qu and Thomas (*22*).

Addition of PS membranes to either wild-type or mutant NBF-1 results in slight quenching and a blue-shift of 3−4 nm for the wild-type and 1−2 nm for the mutant (see Figure 1a−c). However, when PC membranes were added, both species exhibited an enhanced quantum yield with no detectable shifts in emission maxima. These results indicate that when either mutant or wild-type NBF-1 species interacts with PS membranes, the tryptophan 496 then resides in an even more hydrophobic environment. On the other hand, although both protein species interact with PC membranes, as manifested by the increased quantum yield, there is no apparent consequence for the hydrophobicity of the tryptophan environment.

The membrane-induced conformational changes in NBF-1 were further tested by analysis of tryptophan fluorescence quenching by acrylamide (Figure 1d−f). We found that in the absence of phospholipids, acrylamide, a polar collisional quencher, quenched the tryptophan fluorescence of both the wild-type and mutant NBF-1 molecules with similar efficacy as evidenced by the Stern−Volmer constant (K_{S-V}) (Figure 1f). These constants, given by the slopes of the plots in Figure 1 (panels d and e), are sensitive quantitative measures of quencher accessibility to the fluorophore. As expected, denaturation by 8 M urea substantially enhanced tryptophan accessibility to acrylamide quenching in both species.

As shown in Figure 1d, the ability of acrylamide to quench the tryptophan fluorescence of wild-type NBF-1 was significantly suppressed in the presence of PS but not PC membranes. Quantitatively, the presence of PS resulted in the reduction of the Stern−Volmer constant by nearly 2-fold, while PC effects were insignificant (see Figure 1f). However, in the case of the mutant NBF-1, acrylamide quenching was significantly suppressed by both PS and PC membranes (Figure 1e,f). Thus, PS and PC interact with both wild-type and mutant NBF-1, but only PS protects the W496 in the wild-type protein against acrylamide quenching. By contrast, the ΔF508 mutation allows both PS and PC to protect the tryptophan from accessibility to the aqueous quencher. These data thus suggest that the ΔF508 mutation results in a conformational change, which permits the NBF-1 to more profoundly penetrate through an uncharged lipid-headgroup layer than it otherwise might in the wild-type conformation.

Circular Dichroism Studies of Wild-Type and of Mutant NBF-1 Domains. We therefore turned our attention to the questions of whether NBF-1 and NBF-1(ΔF508) might differ in secondary structure, and whether selective phospholipid binding to the NBF-1 might manifest further structural changes. Based on inspection of the circular dichroism (CD) spectra (see Figure 2), and on modeling using both the CONTIN method (*23*) and the method of Yang (*24*), we noted that the structures of both mutant and wild-type NBF-1 molecules had substantial β-pleated sheet components (30−52%). However, as shown in Figure 2, the ΔF508 mutant was less structured than the wild-type by ca. 23%. These data, as well as the α helical content, in the range of 9−15%, are in agreement with the results reported by others for recombinant NBF-1 (*25*) and for a fusion protein of NBF-1

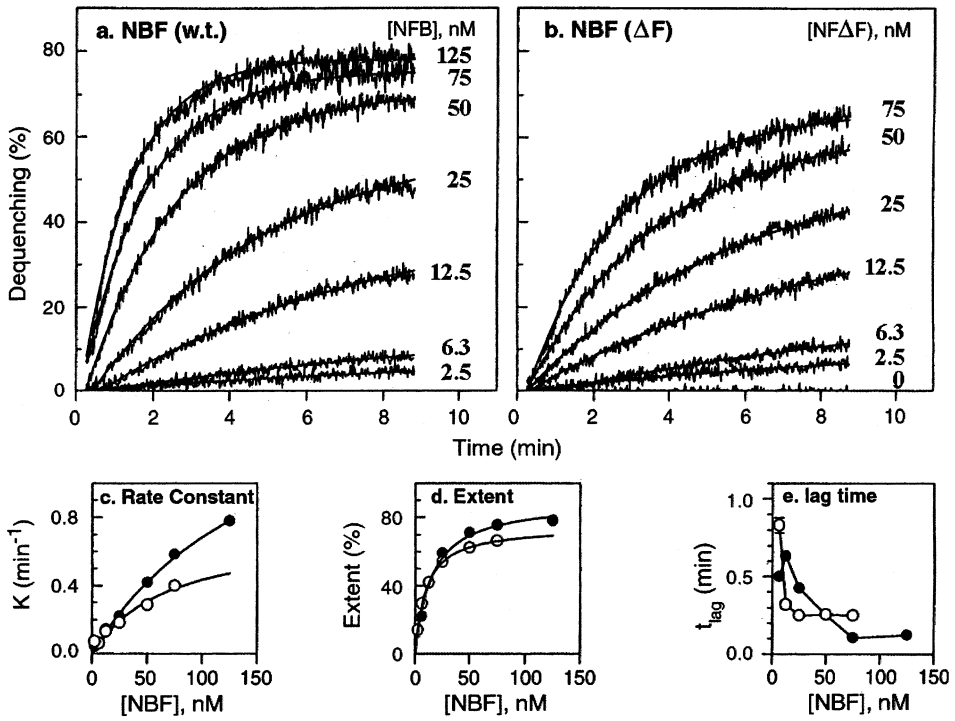

FIGURE 3: Membrane permeabilization of large unilamelar vesicles (LUV) induced by NBF-1 and NBF-1(ΔF508). PS-LUV (300 nM PS) loaded with calcein were exposed to the amounts of NBF-1 (a) or NBF-1(ΔF508) (b) shown in the figure. The experimental data (dotted lines) were fitted to eq 2 **(**solid lines).

with the maltose binding protein (*26*). In addition, these results are consistent with data showing structural differences between "wild-type" p67 and "mutant" p66 peptides from NBF-1 (*27*).

According to the CONTIN method, this difference between mutant and wild-type NBF-1 structure might be traced to a slightly larger α helical component in the wild-type molecule. However, addition of either PC or PS resulted in an enhanced α helical content at the expense of β sheet structure, leading to similar levels of ellipticity for both mutant and wild-type proteins. We also measured the CD spectra in membrane-mimetic environments such as trifluoroethanol (TFE) and sodium dodecyl sulfate (SDS). Addition of 94% TFE raised the computed α helical content from 9−15% to 32−39%, with no significant difference noted between mutant and wild-type NBF-1. SDS, in molecular (0.1%) or micellar (1%) forms, also raised the α helical content to similar levels in both wild-type and mutant proteins, but with less efficiency than TFE. Thus, significant changes in the α helix content can be induced in the wild-type and mutant NBF-1 molecules by either phospholipids or selective membrane-mimetic purturbants. We therefore conclude, as anticipated from the fluorescence data, that the CD data do confirm the fact that both PS and PC change the secondary structure of NBF-1 in subtle but distinct ways.

Liposome Permeability Changes Induced by Wild-Type or Mutant NBF-1 Domains. Turning now to the question of whether the ΔF508 mutation might have functional consequences, we compared the ability of wild-type or mutant NBF-1 to cause the release of an encapsulated impermeable solute, calcein, from liposomes. For this purpose, we prepared large unilamellar vesicles (LUV) of PS or PC encapsulating calcein at a self-quenching concentration, and allowed these vesicles to interact with either wild-type or mutant NBF-1. As shown in Figure 3a,b, increasing concentrations of both NBF-1 species indeed caused a progressive increase in the rate of release of entrapped calcein within the PS liposomes. At lower concentrations of protein, the progress of the efflux reaction showed a brief lag, followed by an apparent first-order increase. With increasing concentrations of protein, the lag phase became shorter, and the rate of efflux increased. The whole reaction was found to be accurately modeled by an equation containing a first-order exponential with rate constant k (Figure 3c), following a lag time t_{lag} (Figure 3e):

$$F(t) = F_{\infty}\{1 - e^{-k(t-t_{lag})}\} \qquad (2)$$

The fitted curves are the solid lines superimposed on the experimental data in Figure 3a,b. The kinetics of these reactions depict saturating processes which indicate that NBF-1 binds to the PS membranes. Since it is likely that the lag time represents the time needed to assemble NBF-1 molecules into polymeric species at the membrane, it is possible that dye release occurs only when the liposome binds a minimal number of NBF molecules. The saturation data also support the concept that NBF-1 molecules do not redistribute rapidly between different vesicles. In this process, the wild-type and mutant NBF-1 molecules are distinguished from one another by rate constants (Figure 3c), extents (Figure 3d), and lag times (Figure 3e). Fundamentally, the effect of the ΔF508 mutation is to *decrease* the probability of NBF-1 inducing release of the anionic dye from PS vesicles.

To investigate the efflux specificity of wild-type and ΔF508 NBF-1 for PS and PC phospholipids, we reacted both NBF species with calcein-loaded liposomes composed of various proportions of PS and PC. Figure 4 a,b shows that both wild-type and mutant NBF-1 molecules substantially

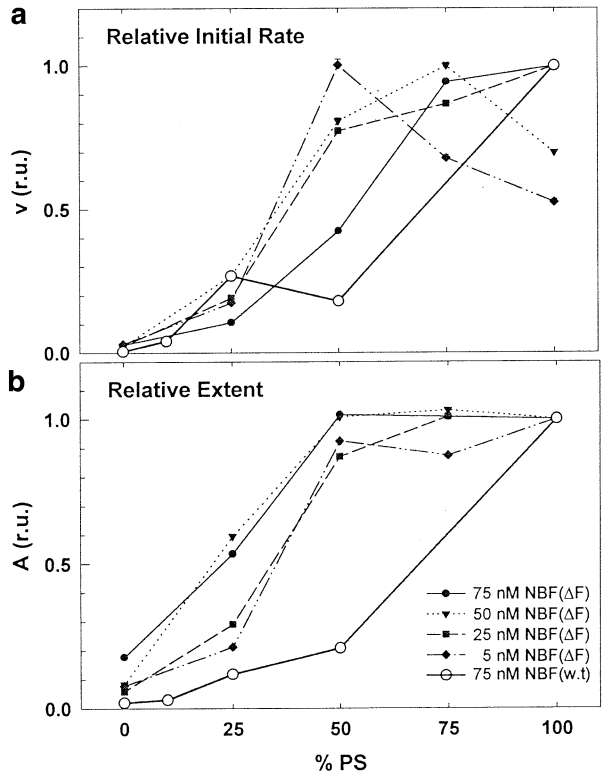

FIGURE 4: Differential capacity of wild-type or ΔF508 NBF-1 to induce calcein efflux from phosphatidylserine (PS) or phosphatidylcholine (PC) large unilamellar vesicles. (a) Relative initial rates of calcein release by NBF-1 or NBF-1(ΔF508) as a function of liposome composition. Percentages (%) refer to proportion of PS in the liposomes made up of a mixture of PS and PC. For the experiments with wild-type NBF-1, the protein concentration is 75 nM and the lipid concentration 220 nM. For the experiments with mutant NBF-1, the protein concentration is as indicated, between 5 and 75 nM, and the lipid composition is 160 nM. Error bars are for the most part smaller than the size of the symbols. (b) Relative extents of calcein efflux are shown for the experiments described in part a.

prefer to induce calcein efflux from pure PS rather than pure PC vesicles. Indeed, the membranes containing only PC show virtually no efflux upon the addition of wild-type NBF-1, and only slight release upon the addition of the mutant NBF-1. However, the mutant NBF-1 is much more tolerant to admixtures of PC with PS than is the wild-type molecule. For example, a 50% replacement of PS by PC results in an ca. 80% loss of efflux activity with wild-type NBF-1. Nonetheless, under the same phospholipid replacement conditions with different concentrations of the ΔF508 mutant, essentially no loss in potency is observed in either the initial rate or the extent of the efflux reaction.

These data thus give further support to the concept that NBF-1 can bind specifically to lipid bilayers, and that the ΔF508 mutation influences the interaction. Furthermore, the ability of the mutation to expand the membrane interactions of NBF-1 to include PC, as shown by protection from acrylamide quenching of W496, coincides faithfully with functional consequences for the formation of a calcein efflux pathway in liposomes. Thus, if these conclusions were indeed important for CFTR trafficking in vivo, one might usefully entertain the hypothesis that defective trafficking of ΔF508-CFTR might be traced to preferential interactions between mutant CFTR and phosphatidylcholine.

Influence of Lipid Composition on Trafficking of Wild-Type or Mutant CFTR in Vivo. To test this "phospholipid chaperone" hypothesis directly, we have grown L-cells expressing either wild-type or ΔF508-CFTR in media in which choline is replaced with a variety of uncharged choline analogues. Under these conditions, the cells replace large fractions of the neutral phospholipid PC with phospholipid analogues whose headgroups correspond to the analogue supplement (*20*). The choline analogues we chose to study were 2-aminobutanol (AB), methylethanolamine (MEA), and 3-aminopropanol (AP). Glaser et al. (*20*) had shown that over a 3 day culture period, these analogues caused reductions of PC from 51.8% of total phospholipids to 17.8% (AP supplement), 15.2% (MEA supplement), and 11.1% (AB supplement). In each case, PC was replaced quantitatively by the corresponding acidic phospholipid: either phosphatidyl-AP, phosphatidyl-MEA, or phosphatidyl-AB (see Figure 5).

As shown in Figure 6 A,D, L-cells expressing wild-type CFTR responded to the various supplements with either little change (+AB) or reductions (+MEA, +AP) in CFTR. As expected, very little CFTR was detected in unsupplemented cells expressing mutant CFTR. However, as shown in Figure 6B,E, supplemented mutant cells expressed more CFTR, with MEA supplementation the most robust. In a separate experiment in which the MEA concentration was titrated (see Figure 6C), the optimal MEA concentration was ca. 50 μM. In addition to the increase in total CFTR, several high molecular weight CFTR bands were detected which increased in a dose-dependent manner (see Figure 6F). Among the important positive controls in this experiment was the use of a different monoclonal antibody (anti-NBF-1 from Dr. Norbert Kartner), which gave virtually identical results to those with the anti-C-terminal domain antibody from Genzyme. These data thus clearly indicate that choline replacement differentially affects the apparent trafficking and stability of wild-type and mutant ΔF508-CFTR's. We therefore interpret these data as providing strong support for the phospholipid chaperone hypothesis.

In addition to the biochemical evidence shown above of increased CFTR maturation, we used confocal microscopy to assess how choline analogues affected the expression and trafficking of wild-type or ΔF508-CFTR in recombinant L-cells. Figure 7 shows the effects of MEA on the expression levels and cellular distribution patterns of ΔF508-CFTR by depicting the level of CFTR in a series of *z*-axis optical sections in cells treated with MEA for 2 days. The control (no MEA) cells show low levels of CFTR, with, at most, slightly increased perinuclear labeling. MEA-treated cells, on the other hand, show enhanced cytoplasmic labeling with a punctuated pattern while the nuclear and plasma membrane regions are at background levels. This pattern, together with the glycosylation data, suggests that MEA promotes survival of mutant CFTR proteins.

Since confocal microscopy shows the effect at a few selected fields, we opted to enhance the statistical significance of the confocal microscopy data by studying the entire ensamble of cells using cell cytometry. For this purpose, we studied MEA-treated CFTR-transfected L-cells using scanning laser cytometry. Figure 8 shows the histograms of the distribution of integrated fluorescence intensity in these cells.

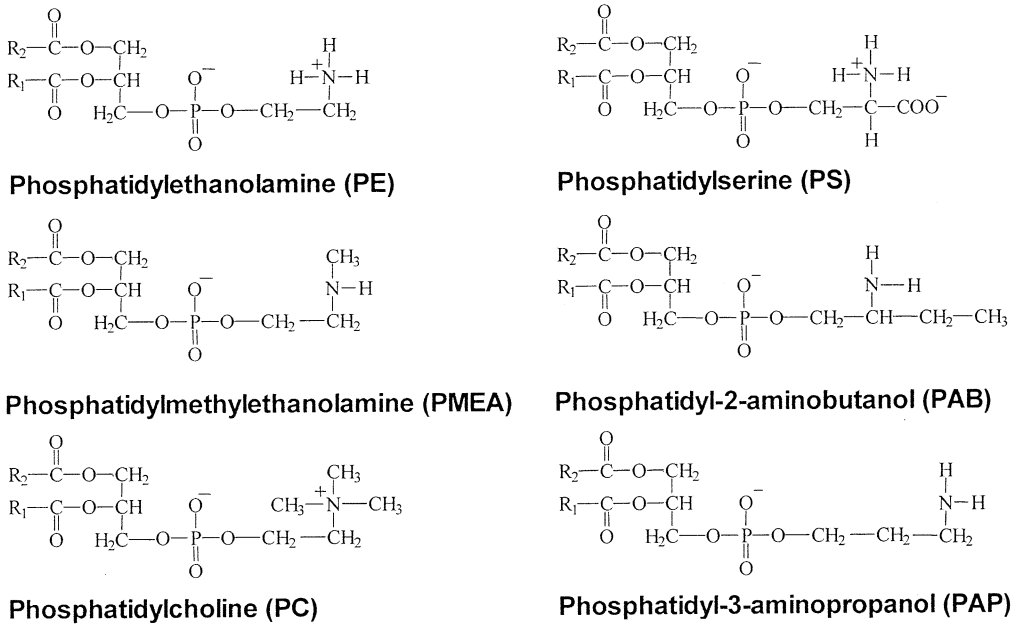

FIGURE 5: Structures of the phosphatidylcholine (PC) analogues.

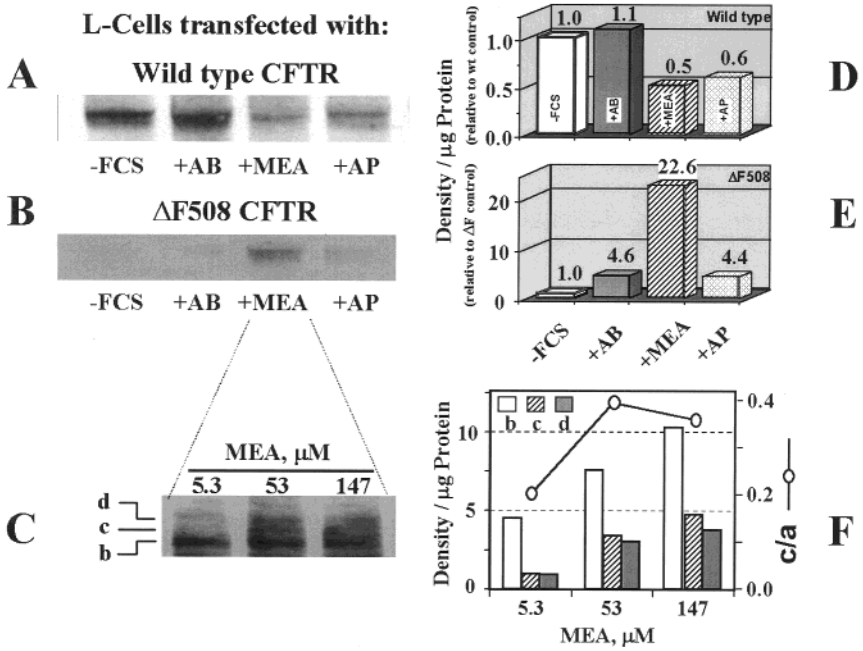

FIGURE 6: Effect of choline analogues on ΔF508-CFTR trafficking in vivo as evidenced by CFTR glycosylation. Western blot of membranes from L-cells expressing wild-type CFTR (A) or ΔF508-CFTR (B). Cells were cultured in the absence of fetal calf serum (−FCS) to avoid adding choline, and supplemented with 40 μg/mL (53 μM) of either 2-aminobutanol (AB), methylethylamine (MEA), or 3-aminopropanol (AP). (C) Titration of the effect of MEA on ΔF508-CFTR expressed in L-cells. The lower case letters a, b, and c indicate various molecular weight CFTR bands which may be equivalent to the conventional glycosylated bands of wild-type CFTR. Densitometry of CFTR-positive immunoreactivity for wild-type (D) or mutant (E) CFTR transfected cells. The integrated intensity in each band in part A was corrected for the amount of protein loaded in the lane, and normalized to the respective controls (−FCS). The total immunoreactive density is used for the calculation. (F) Relative densitometric expression of ΔF508-CFTR-positive immunoreactivity from cells incubated in different concentrations of MEA. Bands a, b, and c correspond to equivalently labeled bands in part C. The ratio of c/a is calculated from the individual bar graph values.

In control ΔF508-CFTR-transfected L-cells, not treated with MEA, most of the cells show a low level of labeling by fluorescent antibodies with very few cells having high intensity. However, when grown in the presence of MEA, a large proportion of the same cells display high labeling. In contrast, untreated wild-type CFTR-transfected L-cells mostly show a high level of labeling. MEA treatment seems to somewhat lessen the expression of wild-type CFTR in transfected L-cells, but the vast majority of the population still distributes in the high-intensity peak.

DISCUSSION

These data show that the ΔF508 mutation in NBF-1 allows PC into a domain near ΔF508 and W496 that was not previously permitted in the wild-type conformation. This effect of the ΔF508 mutation on NBF-1 may have patho-

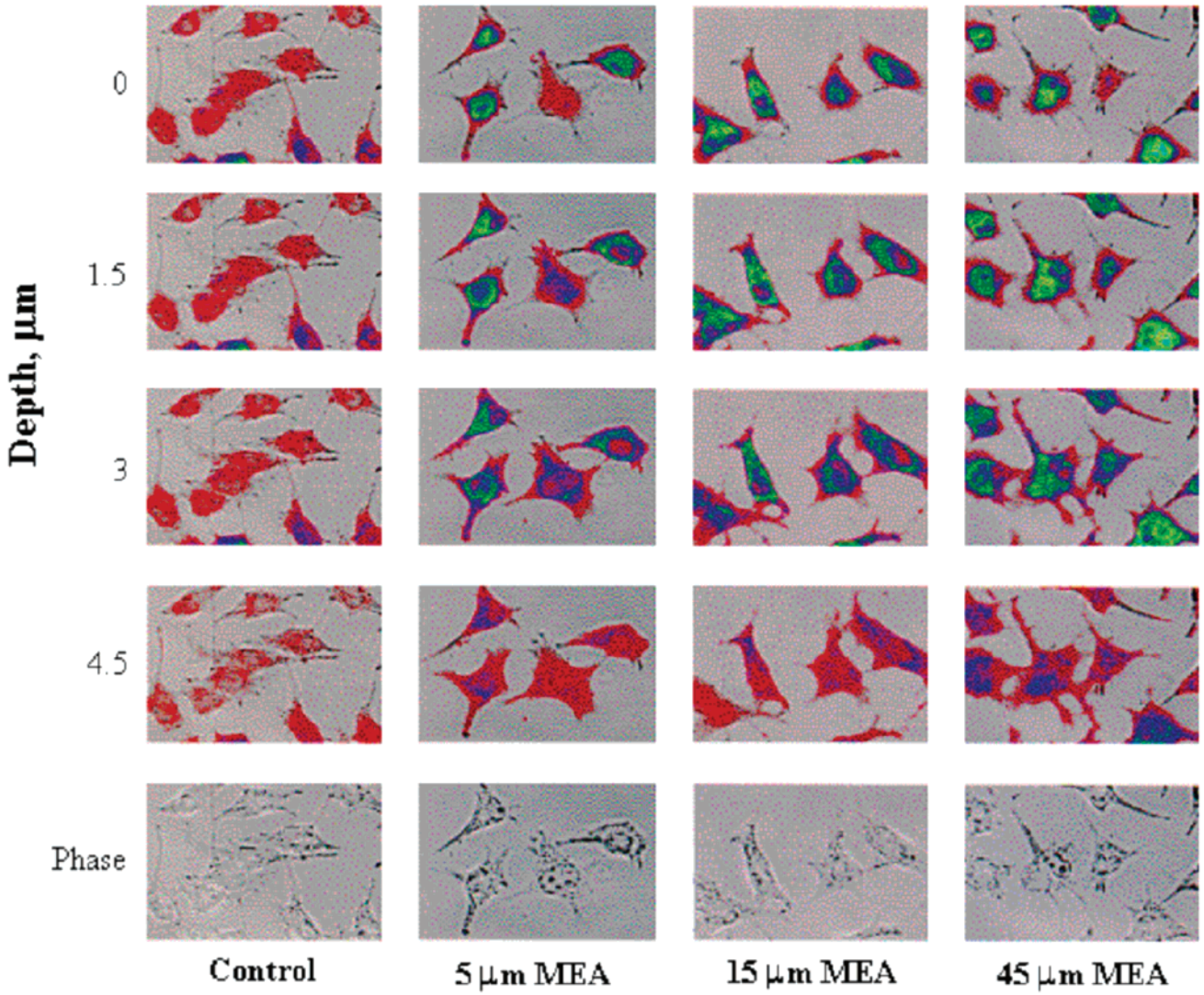

FIGURE 7: Confocal microscopy evidence for the potentiation of ΔF508-CFTR trafficking in vivo by choline analogues. Confocal fluorescence intensity images of CFTR-transfected L-cells grown in the absence or presence of the indicated concentration of MEA and probed with FITC-labeled secondary antibodies to anti-CFTR monoclonals. Images are shown in false color as a function of the depth in *z*-series. The bottom row shows the phase image for the same field.

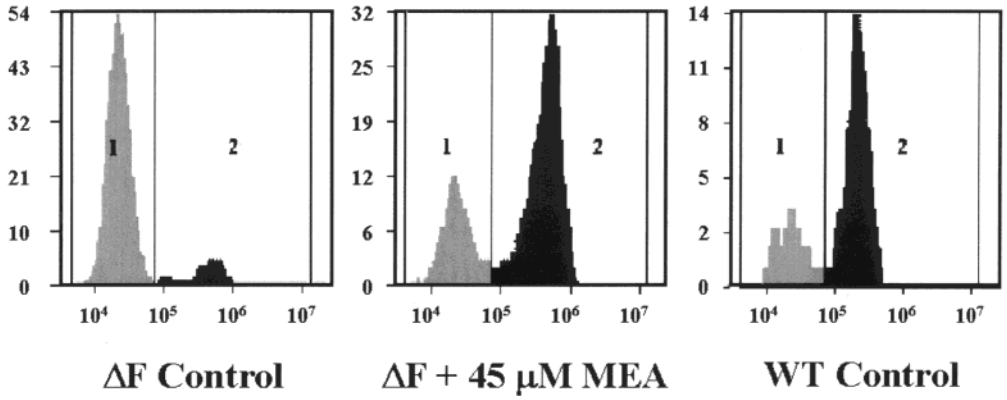

FIGURE 8: Evidence for the effect of choline analogues on the trafficking of ΔF508-CFTR in vivo by laser scanning cytometry. Distribution of cellular FITC fluorescence intensities for CFTR-transfected L-cells grown on microscope slides in the presence or absence of 45 μM MEA and labeled with FITC-tagged secondary antibodies to anti-CFTR monoclonal antibodies.

physiological significance for cystic fibrosis, since reduction in cellular PC and replacement by noncharged analogues appear to have an ameliorating effect on defective mutant CFTR trafficking in vivo. This is evidenced by increased expression of ΔF508-CFTR (Figures 6−8) and enhancement of higher molecular weight CFTR components (Figure 6). Previous studies have suggested that recognition of the mutant CFTR by proteins in the family of chaperonins (*5*−*12*) could lead to degradation by the proteosome system (*11*, *12*). However, since PC and PS are distributed asymmetri-

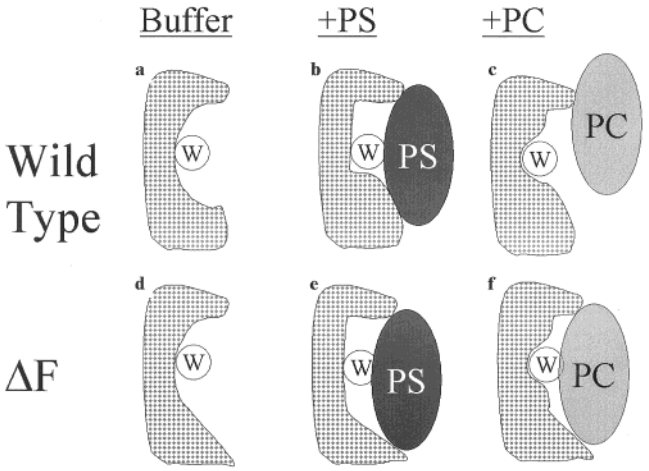

FIGURE 9: Models for the interaction of phosphatidylserine and phosphatidylcholine with wild-type and mutant NBF-1. (a) For wild-type (wt) NBF-1, the tryptophan 496 ("W") is depicted as residing in a hydrophobic pocket, as defined by the fluorescence spectrum. (b) In the presence of PS, the global secondary structure of wild-type NBF-1 molecules changes, and the hydrophobicity of the pocket enveloping the W496 is enhanced. Furthermore, the tryptophan is protected from quenching by acrylamide by PS interacting in the vicinity of the tryptophan. (c) In the presence of PC, the global conformation of wild-type NBF-1 is also changed, but with significant differences. Not only does the tryptophan fail to be blue-shifted, but also the quantum yield is actually somewhat enhanced. Furthermore, PC fails to provide protection to W496 from acrylamide quenching. For that reason, the conformation in the vicinity of W496 is shown with a different structure from that with PS in part b. (d) For mutant NBF-1, the tryptophan 496 ("W") resides in a hydrophobic pocket, which is slightly less polar (by fluorescence) and less structured (by CD) than the wild-type molecule (cf. part a). (e) In the presence of PS, the global secondary structure of mutant NBF-1 molecules changes, and the hydrophobicity of the pocket enveloping the W496 is enhanced. Furthermore, the tryptophan is protected from quenching by acrylamide. These changes are similar to those for wild-type NBF-1, and so the structure around the W496 is shown with a similar shape. (f) However, in the presence of PC, the tryptophan of the mutant NBF-1 becomes shielded from quenching by acrylamide. For that reason, the shape of the structure enclosing W496 is shown different from the structure in part c, and PC is shown to bind in a different position to the mutant than in the wild-type NBF-1 shown in part c.

cally in the endoplasmic reticulum, it is also possible that aberrant interactions between the NBF-1 domain of CFTR and phospholipids could also contribute to the processing defect. Phospholipid chaperones have been previously demonstrated for the lac permease system (*17*, *18*), indicating that the concept is not unique to the CFTR system.

The mechanism underlying these effects of phospholipids on mutant CFTR processing may be explained by the biophysical results from studies on wild-type and mutant NBF-1. From these studies, it is evident that the site of lipid interaction with NBF-1 is in the vicinity of the tryptophan at position 496. Not only do the lipids change the spectral properties of the lone tryptophan in different ways (Figure 1a−c), but also PS influences the accessibility of the tryptophan to an aqueous quencher in preference to PC (Figure 1d−f). These data are supported by the observation from CD studies that both lipid types cause changes in the secondary structure of NBF-1. In parallel to these observations, the wild-type NBF-1 promotes the efflux of the anionic dye calcein from PS liposomes but not from PC liposomes.

The ΔF508 mutation in NBF-1 causes subtle, systematic changes in the structure of the protein and in the nature of interactions with phospholipids. In addition to the intrinsic changes in fluorescence and CD spectra of the protein (Figures 1a−c and 2), the ΔF508 mutation leads to conformational changes, which permit both PS and PC to protect W496 from acrylamide quenching. Furthermore, the ΔF508 mutation not only decreases the rate of calcein efflux from PS liposomes, but also renders the efflux process more tolerant to PC in the system. Thus, the changes in the nature of the interaction of PC with mutant NBF-1, noted at the molecular level by the tryptophan at position 496, are faithfully reproduced at the functional level by efflux of the anionic dye calcein from liposomes. In addition, these data further specify the conclusion that phospholipid interactions with NBF-1 occur at or near a site influenced by the F508 residue. We summarize these results with the models in Figure 9, in which tryptophan 496 ("W") is depicted within a hydrophobic pocket in the NBF-1 molecules, and PC and PS are represented only by general ellipses to avoid speculation about molecular orientation.

In conclusion, we have found that the recombinant wild-type NBF-1 domain interacts selectively with phosphatidylserine (PS) rather than phosphatidylcholine (PC), in vitro. By contrast, NBF-1 carrying the ΔF508 mutation loses the ability to discriminate between the two types of phospholipids. In vivo, in cells expressing ΔF508-CFTR, replacement of PC by noncharged analogues results in an absolute increase in CFTR, and a progressive expression of higher molecular weight CFTR forms. Thus, phospholipid chaperones may be important for CFTR trafficking, and contribute to the pathology of cystic fibrosis.

ACKNOWLEDGMENT

We acknowledge useful suggestions from Dr. George Lee (NIH) and Mr. Hung Cahouy (USUHS) and helpful discussions with Dr. Anne Walter (St. Olaf).

REFERENCES

1. Kerem, B.-S., Rommens, J. M., Buchanan, J. A., Markiewicz, D., Cox, T. K., Chakravarti, A., Buchwald, M., and Tsui, L.-C. (1989) Identification of the cystic fibrosis gene: genetic analysis. *Science 245*, 1073−1080.
2. Riordan, J. R., Rommens, J. M., Kerem, B.-S., Alon, N., Rozmahel, R., Grzelczak, Z., Zielenski, J., Lok, S., Plavsic, N., Chou, J. L., Drumm, M. L., Iannuzzi, M. C., Collins, F. S., and Tsui, L.-C. (1989) Identification of the cystic fibrosis gene: Cloning and characterization of complementary DNA. *Science 245*, 1066−1073.
3. Rommens, J. M., Iannuzzi, M. C., Kerem, B.-S., Drumm, M. L., Melmer, G., Dean, M., Rozmahel, R., Cole, J. L., Kennedy, D., Hidaka, N., Zsiga, M., Buchwald, M., Riordan, J. R., Tsui, L.-C., and Collins, F. S. (1989) Identification of the cystic fibrosis gene: Chromosome walking and jumping. *Science 245*, 1059−1065.
4. Welsh, M. J., Tsui, L. C., Boat, T. F., and Beaudet, A. L. (1995) Cystic fibrosis. in *The metabolic and molecular bases of inherited disease* (Scriver, C. L., Beaudet, A. L., Sly, W. S., and Valle, D., Eds.) Seventh ed., pp 3799−3876, McGraw-Hill, New York.
5. Cheng, S. H., Gregory, R. J., Marshall, J., Paul, S., Souza, D. W., White, G. A., O'Riordan, C. R., and Smith, A. E. (1990) Defective intracellular transport and processing of CFTR is the molecular basis of most cystic fibrosis. *Cell 63*, 827−834.
6. Denning, G. M., Ostedgaard, L. S., and Welsh, M. J. (1992) Abnormal localization of cystic fibrosis transmembrane conductance regulator in primary cultures of cystic fibrosis airway epithelia. *J. Cell Biol. 118*, 551−559.
7. Denning, G. M., Ostedgaard, L. S., Cheng, S. H., Smith, A. E., and Welsh, M. J. (1992) Localization of cystic fibrosis transmembrane conductance regulator in chloride secretory epithelia. *J. Clin. Invest. 89*, 339−349.

8. Kartner, N., Augustinas, O., Jensen, T. J., Naismith, A. L., and Riordan, J. R. (1992) Mislocalization of ΔF508 CFTR in cystic fibrosis sweat gland. *Nat. Genet. 1*, 321−327.
9. Lukacs, G. L., Mohamed, A., Kartner, N., Chang, X. B., Riordan, J. R., and Grinstein, S. (1994) Conformational maturation of CFTR but not its mutant counterpart (delta F508) occurs in the endoplasmic reticulum and requires ATP. *EMBO J. 13*, 6076−6086.
10. Ward, C. L., and Kopito, R. R. (1994) Intracellular turnover of cystic fibrosis transmembrane conductance regulator. Inefficient processing and rapid degradation of wild-type and mutant proteins. *J. Biol. Chem. 269*, 25710−25718.
11. Ward, C. L., Omura, S., and Kopito, R. R. (1995) Degradation of CFTR by the ubiquitin-proteasome pathway. *Cell 83*, 121−127.
12. Jensen, T. J., Loo, M. A., Pind, S., Williams, D. B., Goldberg, A. L., and Riordan, J. R. (1995) Multiple proteolytic systems, including the proteasome, contribute to CFTR processing. *Cell 83*, 129−135.
13. Arispe, N., Rojas, E., Hartman, J., Sorscher, E. J., and Pollard, H. B. (1992) Intrinsic anion channel activity of the recombinant first nucleotide binding fold domain of the cystic fibrosis transmembrane regulator protein. *Proc. Natl. Acad. Sci. U.S.A. 89*, 1539−1543.
14. Ko, Y. H., Delannoy, M., and Pedersen, P. L. (1997) Cystic fibrosis transmembrane conductance regulator: the first nucleotide binding fold targets the membrane with retention of its ATP binding function. *Biochemistry 36*, 5053−5064.
15. Gruis, D. B., and Price, E. M. (1997) The nucleotide binding folds of the cystic fibrosis transmembrane conductance regulator are extracellularly accessible. *Biochemistry 36*, 7739−7745.
16. Hung, L. W., Wang, I. X., Nikaido, K., Liu, P. Q., Ames, G. F., and Kim, S. H. (1998) Crystal structure of the ATP-binding subunit of an ABC transporter. *Nature 396*, 703−707.
17. Bogdanov, M., Sun, J., Kaback, H. R., and Dowhan, W. (1996) A phospholipid acts as a chaperone in assembly of a membrane transport protein. *J. Biol. Chem. 271*, 11615−11618.
18. Bogdanov, M., and Dowhan, W. (1995) Phosphatidylethanolamine is required for in vivo function of the membrane-associated lactose permease of *Escherichia coli*. *J. Biol. Chem. 270*, 732−739.
19. Chou, P. Y., and Fasman, G. D. (1978) Empirical predictions of protein conformation. *Annu. Rev. Biochem. 47*, 251−276.
20. Glaser, M., Furguson, K. A., and Vagelos, P. R. (1974) Manipulation of the phospholipid composition of tissue culture cells. *Proc. Natl. Acad. Sci. U.S.A. 89*, 4072−4076.
21. Guay-Broder, C., Jacobson, K. A., Barnoy, S., Cabantchik, Z. I., Guggino, W. B., Zeitlin, P. L., Turner, R. J., Vergara, L., Eidelman, O., and Pollard, H. B. (1995) A1 receptor antagonist 8-cyclopentyl-1,3-dipropylxanthine selectively activates chloride efflux from human epithelial and mouse fibroblast cell lines expressing the cystic fibrosis transmembrane regulator ΔF508 mutation. *Biochemistry 34*, 9079−9087.
22. Qu, B.-H., and Thomas, P. J. (1996) Alteration of the cystic fibrosis transmembrane conductance regulator folding pathway. *J. Biol. Chem. 271*, 7261−7264.
23. Provencher, S. W., and Glöckner, J. (1981) Estimation of globular protein secondary structure from circular dichroism. *Biochemistry 20*, 33−37.
24. Yang, J. T., Wu, C. S., and Martinez, H. M. Calculation of protein conformation from circular dichroism. *Methods Enzymol. 130*, 208−269.
25. Logan, J., Hiestand, D., Daram, P., Huang, Z., Muccio, D. D., Hartman, J., Haley, B., Cook, W. J., and Sorscher, E. J. (1994) Cystic fibrosis transmembrane conductance regulator mutations that disrupt nucleotide binding. *J. Clin. Invest. 94*, 228−236.
26. Ko, Y. H., Thomas, P. J., Delannoy, M. R., and Pedersen, P. L. (1993) The cystic fibrosis transmembrane conductance regulator. Overexpression, purification, and characterization of wild type and ΔF508 mutant forms of the first nucleotide binding fold in fusion with the maltose-binding protein. *J. Biol. Chem. 268*, 24330−24338.
27. Thomas, P. J., Shenbagamurthi, P., Sondek, J., Hullihen, J. M., and Pedersen, P. L. (1992) The cystic fibrosis transmembrane conductance regulator. Effects of the most common cystic fibrosis-causing mutation on the secondary structure and stability of a synthetic peptide. *J. Biol. Chem. 267*, 5727−5730.

BI020289S